Int J Adv Manuf Technol (2017) 93:3461–3471
DOI 10.1007/s00170-017-0720-4

ORIGINAL ARTICLE

Optimization of the extrusion die and microstructure analysis for a hollow aluminum alloy profile

Hongxuan Ji[1] · Huixing Nie[2] · Wenlin Chen[1] · Xiangming Ruan[3] · Penglin Pan[1] · Jingwen Zhang[1]

Received: 27 March 2017 / Accepted: 26 June 2017 / Published online: 20 July 2017

Abstract The virtual tryout of the extrusion process of a large hollow aluminum profile is carried out by using numerical simulation. Firstly, a porthole die is designed based on the theory of metal plastic forming, and a finite element model of the extrusion process is established. Following the simulation results, the height and shape of baffle plate are adjusted to balance the material flow velocity in the cross-section of the profile. Through a series of modifications, the standard deviation of the velocity (SDV) at the profile section decreases significantly from 6.1 mm/s that is in the initial state to 3.5 mm/s in the optimum one. Finally, a physical extrusion die is manufactured based on the optimized design, and the extruded profile satisfies the practical requirements. In addition, the microstructure distribution on the product section is analyzed numerically. Results show that the uneven deformation caused by the difference in wall thickness is the main factor that causes the uneven distribution of grain sizes in the cross-section of the product. When the material flows out of the die orifice and undergoes uneven temperature distribution at the profile section, the grain growth rates become different.

Keywords Aluminum profile extrusion · Numerical simulation · Die modification · Microstructure analysis

1 Introduction

Currently, aluminum alloy profiles have been widely used in many fields including construction, rail transportation, aerospace, and large engineering structural components due to their advantages in high specific strength, good corrosion resistance, high surface quality, and good mechanical properties [1–3].

Extrusion process is the key process in the production of aluminum alloy profiles. Proper die design is one of the critical determinant factors to produce high-quality products, especially for large complex industrial aluminum profiles. Up to recently, however, the design of extrusion die is still dependent on imprecise analogy and engineering experience. It is difficult to guarantee the quality of extrusion dies, and numerous "trail-repair" attempts are usually carried out before a satisfactory product is produced. To save the time that is cost on "trail-repair," much attention has been paid on the application of numerical simulation in the extrusion process [3, 4].

Lee et al. [5] have analyzed the extrusion process for the automobile condenser tubes based on the finite element software. The effects of the welding chamber structure on material flow, welding pressure, extrusion load, and the elastic deformation of mandrel have been evaluated. Based on the numerical analysis software Msc/SuperForge, Wu et al. [6] have simulated the

✉ Wenlin Chen
wlchen8761@126.com

Hongxuan Ji
1206830863@qq.com

[1] School of Materials Science and Engineering, Hefei University of Technology, Hefei, Anhui 230009, People's Republic of China

[2] School of Management, Hefei University of Technology, Hefei 230009, Anhui, People's Republic of China

[3] Anhui Shengxin Aluminum Corporation Limited, Xuancheng 242000, Anhui, People's Republic of China

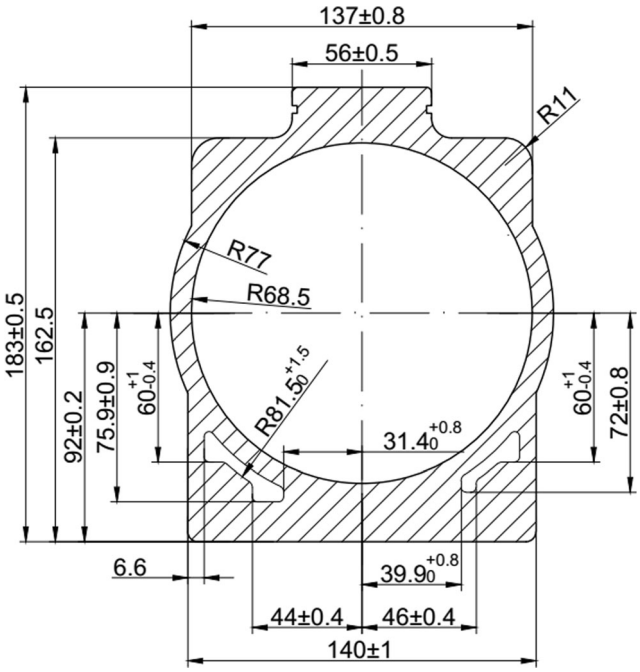

Fig. 1 Cross-section shape and dimensions of the profile (mm)

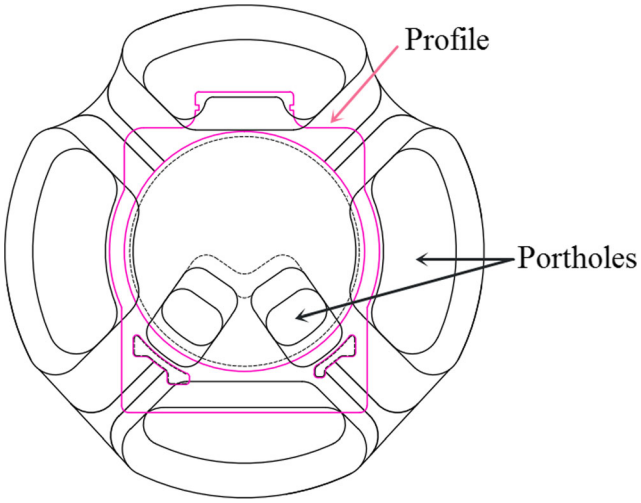

Fig. 3 The arrangement of the portholes and profile

extrusion process for the aluminum rectangular hollow pipe. The optimal die design scheme has been obtained by adjusting the size, shape, and position of portholes and welding chamber, as well as the local bearing lengths, etc. In order to investigate the effects of pockets on material flow, temperature at the bearing exit and extrusion load, He et al. [7] designed two different multi-hole porthole dies with and without pockets. The simulation results showed that the pockets could be used to effectively adjust the metal flow, especially it is beneficial to the metal flow under the legs. Dong et al. [8] have obtained the constitutive equation and processing maps of Al–Mg–Si aluminum alloy by hot compression test. The identified material parameters and processing parameters were applied to simulate the extrusion process of a complex cross-section profile used in manufacturing of high-speed train body. By adding baffle plates and adjusting bearing lengths, the velocity uniformity was improved greatly, and the profile was finally extruded with desired size and geometry. Based on the arbitrary Lagrangian-Eulerian code HyperXtrude, Zhang et al. [9] transferred the "trial-repair" process of the extrusion die from the workshop to the computer to design a complex hollow aluminum profile used in high-speed trains. To balance the material flow velocity in the die cavity, more than ten baffle plates were used and distributed in the welding chamber. Finally, a real extrusion die was manufactured according to the optimal design, and the extruded profile could satisfy the practical requirements. The virtual tryout and design rules of extrusion dies could provide theoretical guidance for practical repairs of complex extrusion dies in workshop.

In summary, many scholars have carried out a lot of investigations on the extrusion process of aluminum alloy profiles and die optimization. With the applications becoming complex, multi-cavity aluminum profiles in the industrial field continue to expand. Meanwhile, the

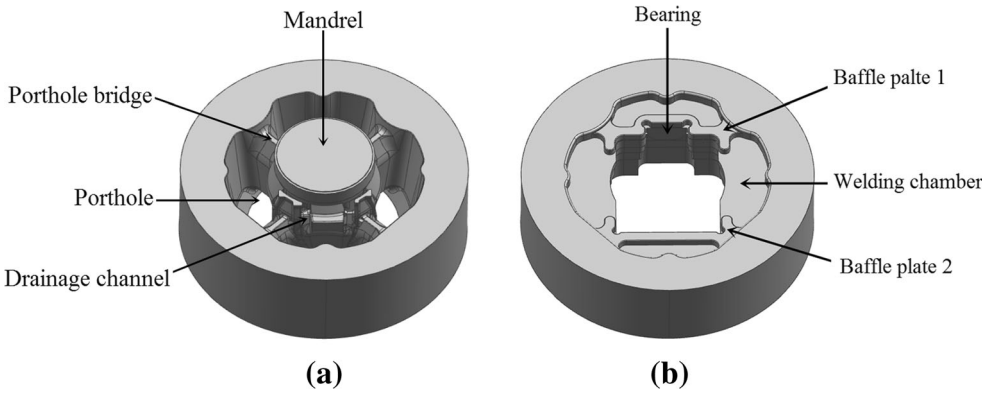

Fig. 2 3D model of the initial extrusion die. **a** Upper die. **b** Lower die

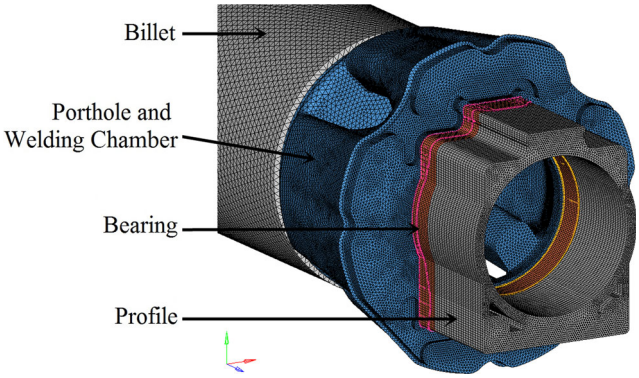

Fig. 4 Numerical analysis model

material flow in the extrusion process becomes more complicated and the actual "trail-repair" process for designing extrusion dies is especially time wasting and inefficient. For these reasons, the finite element analysis method will be adopted to simulate the extrusion process for a hollow aluminum profile with a large difference in wall thickness. By adjusting the position, shape, and size of baffle plate, the material flow will be analyzed and the extrusion die will be modified. In addition, the microstructure distribution on the product section will be analyzed by means of the numerical simulation technique.

2 Numerical simulation models

2.1 The initial die structure and geometry

The cross-section shape and dimensions of the hollow aluminum profile studied in this work are shown in Fig. 1. This profile has three cavities, i.e., a circular cavity on the upper location and two small cavities beneath the former one. The section size of the profile is 140 mm × 183 mm, with minimum and maximum wall thicknesses of 6.6 and 23.8 mm, respectively. Due to its complex shape in cross-section and large difference in wall thickness, it is difficult to control the velocity uniformity in the cross-section of the profile. The section area of the profile is 9162.8 mm^2, and the maximum inscribed circle diameter is about 210 mm. The extrusion process can be accomplished on a 25 MN extrusion machine according to the largest inscribed circle diameter [10]. Correspondingly, the inside diameter of container is 232 mm and the billet diameter is 222 mm, with a height of 800 mm, making the extrusion ratio to be 4.28.

The porthole die is applied to produce this profile and the initial die structure is shown in Fig. 2. Fig. 2a is the upper die, with an outer diameter of 397 mm and a height of 195 mm. In order to control the material distribution and balance the metal flow reasonably, six portholes are designed, of which the arrangement and profile is shown in Fig. 3. To ensure adequate material supply between the cavities, two small portholes and drainage channels are adopted to guide material flowing into the area. Figure 2b shows the lower die, with an outer diameter of 397 mm and a height of 105 mm. According to the container diameter, the welding depth is designed as 35 mm, and the height of welding chamber in lower die is 15 mm [11].

2.2 Mesh model

All the regions that material flows through are extracted to create a simplified model, including billet, porthole, welding chamber, bearing, and profile as shown in Fig. 4. For the reasonable control of the element number and calculation accuracy, different types and sizes of elements are assigned at various parts of the numerical

Table 1 Main thermal and mechanical parameters of the AA6063 and H13

Material	Mass density (kg/m^3)	Specific heat ($N/(mm^2\ K)$)	Thermal conductivity (N/(s K))	Coefficient of thermal expansion (1/K)	Young's modulus (Pa)	Poisson's ratio
AA6063	2700	900	198	1.0×10^{-5}	4.0×10^{10}	0.35
H13	7870	460	24.3	–	2.1×10^{10}	0.35

Table 2 Process parameters used in the simulation

Parameters	Initial temperature of billet (K)	Initial temperature of die (K)	Initial temperature of container (K)	Rem speed (mm/s)
Values	773	743	693	10

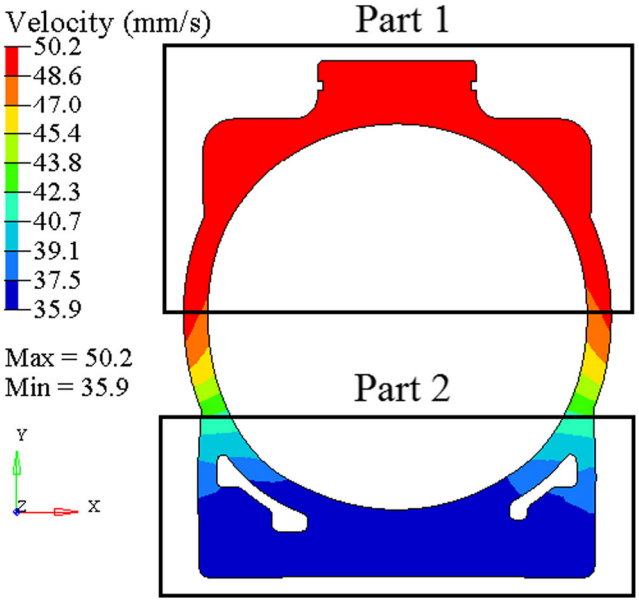

Fig. 5 Velocity distribution in the cross-section with the initial extrusion die

analysis model. Since the bearing region is mainly subjected to severe shear deformation to form the final shape of the profile, the finer triangular prism elements are adopted in the regions of bearing and profile. Meanwhile, the relatively coarse tetrahedral elements are used in the regions of porthole, welding chamber, and billet. The total number of the numerical model is about 990,000.

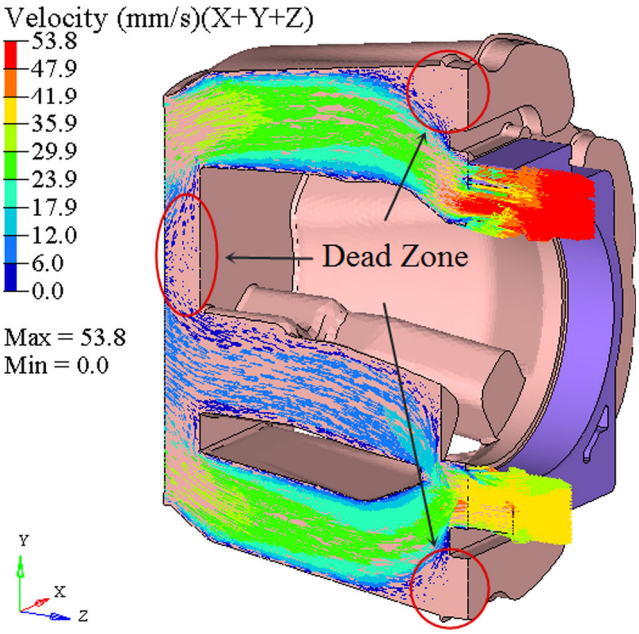

Fig. 6 Velocity distribution in the die cavity with the initial extrusion die

2.3 Material parameters

The billet material is aluminum alloy 6063 and the material for the extrusion die is H13 tool steel. The main thermal and mechanical parameters of the materials used in the present simulation are listed in Table 1. Theoretically, the Sellars-Tegart model can well describe the flow stress of AA6063 [12], which is expressed as:

$$\sigma = \frac{1}{\beta}\sinh^{-1}\left(\frac{Z}{A}\right)^{1/n} \tag{1}$$

where σ is the flow stress, n is a stress exponent, A and β are the temperature independent material parameters and Z is the Zener-Hollomom parameter, as is defined by:

$$Z = \dot{\bar{\varepsilon}} e^{Q/RT} \tag{2}$$

where $\dot{\bar{\varepsilon}}$ is the effective strain rate, Q is the activation energy, R is the universal gas constant, and T is the Kelvin temperature. The values of parameter used for AA6063 in the present simulation are $Q = 1.412 \times 10^9$ J/mol, $R = 8.314$ J/(mol K), $A = 5.91 \times 10^9$ s^{-1}, $n = 5.385$, and $\beta = 4.0 \times 10^{-8}$ m^2/N.

2.4 Boundary conditions and process parameters

The sticking condition is used for all the interfaces between the billet and the tooling (container and die) except at the bearings, while the surfaces in contact with bearings adopt the Coulomb friction condition with a coefficient of 0.3.

The heat transfer coefficient between the billet material and the die is 3000 W/(m^2 K) [13, 14]. The process parameters designed for the simulation are given in Table 2. The established numerical analysis model is shown in Fig. 4.

3 Numerical simulation results and discussion

The velocity distribution in the cross-section of the profile plays an important role in judging the rationality of

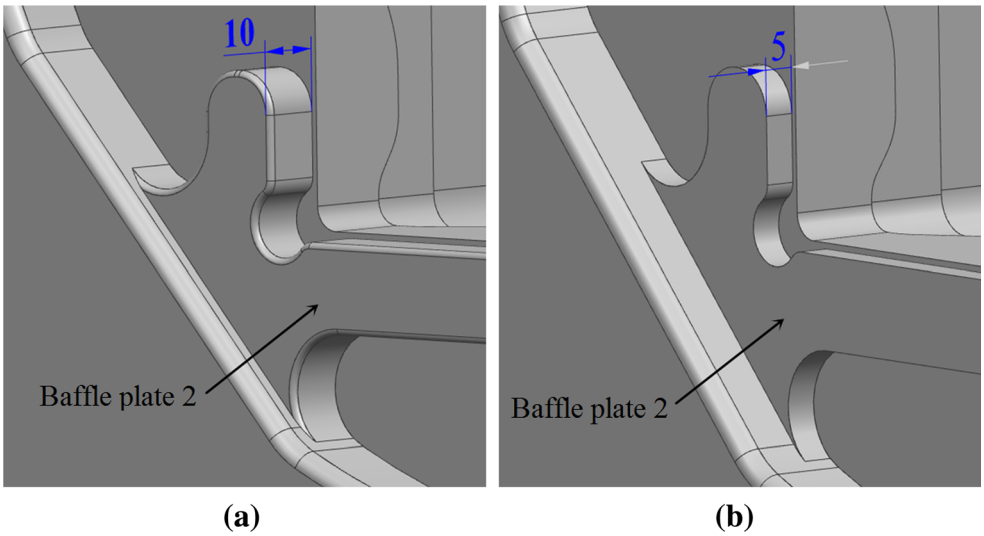

Fig. 7 Height of baffle plate 2 in the first modification scheme. **a** Before modification. **b** After modification (mm)

the die structure and the final product quality and the simulation result is shown in Fig. 5. It is seen that there is a great difference in metal flow velocity in the whole profile section, which can be divided into two parts. Part 1 located in the upper portion of the circular cavity exhibits the maximum velocity. In contrast, the velocity of part 2 under the circular cavity is visibly less than part 1. From part 1 to part 2, the section velocity shows a declining trend, which ranges from 50.2 to 35.9 mm/s.

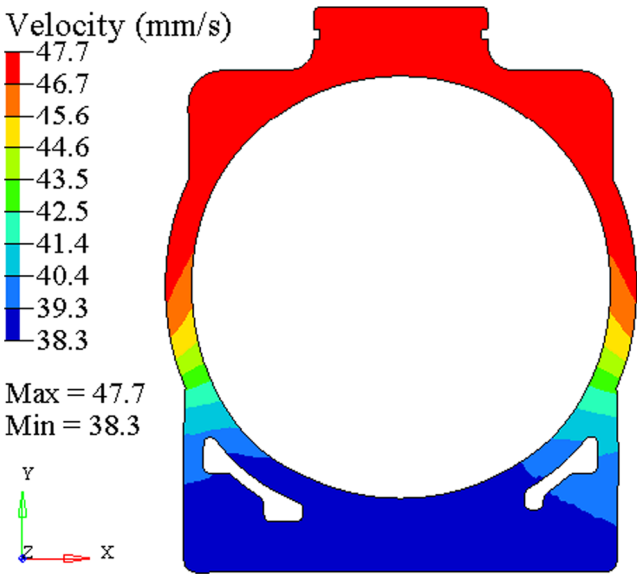

Fig. 8 Velocity distribution in the cross-section with the first modification extrusion die

Figure 6 shows the velocity distribution in the die cavity. As can be seen from Fig. 6, although part of the material is assigned to the two small portholes, the material supply is insufficient. Therefore, the flow velocity is slower than that in other portholes, resulting in a slow welding speed in the region of part 2 that is corresponding to in the welding chamber. Figure 5 reveals the main factor that causes the uneven velocity distribution in the cross-section of the profile.

To accurately judge the extent of velocity uniformity in the cross-section of the profile, the standard deviation of the velocity (SDV) parameter is introduced in this work [15], which can be expressed as:

$$SDV = \sqrt{\frac{\sum_{i=1}^{n}\left(v_i - \overline{v}\right)^2}{n}} \tag{3}$$

where n is the number of nodes in the cross-section of the profile, v_i is the velocity at node i, and $\overline{v}$ is the average velocity of all nodes. It has been confirmed that the smaller SDV values, the more uniform the velocity distribution and the better the quality of the products.

In this work, all nodes in the cross-section have been chosen to calculate the SDV, wherein the initial extrusion die is 6.1 mm/s. Obviously, the initial design scheme of extrusion die is unreasonable for a high SDV value, resulting in some defects as bend and unqualified dimensions of the final product. Therefore, it is necessary to do some modifications of the extrusion die to balance the metal flow velocity.

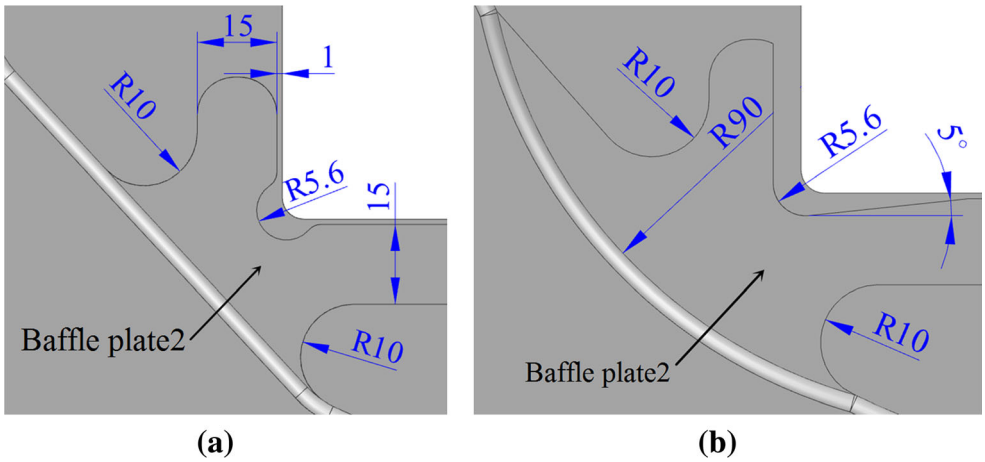

Fig. 9 Shape of baffle plate 2 in the second modification scheme. **a** Before modification. **b** After modification (mm)

4 Modification of the extrusion die

4.1 First modification scheme

According to the velocity distribution in Fig. 5, it is necessary to promote the metal flow of part 2 to improve the velocity uniformity. In the first modification scheme, the height of baffle plate 2, as shown in Fig. 7, is reduced from the original 10 to 5 mm. The extrusion process is simulated again with the same process parameters as the initial model, wherein the velocity distribution of the first modification scheme is shown in Fig. 8. Compared with the initial die structure, the velocity distribution is similar, but the value range of velocity is reduced (47.7–38.3 mm/s). The SDV value is found to be 4.0 mm/s, and there is a 34.4% drop from its initial value of 6.1 mm/s. It is indicated that reducing the height of the baffle plate 2 can significantly improve the velocity uniformity in the cross-section of the profile.

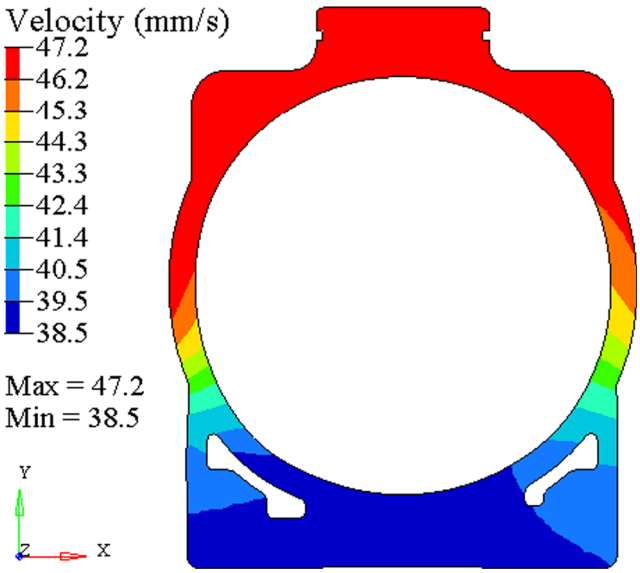

Fig. 10 Velocity distribution in the cross-section with the second modification extrusion die

4.2 Second modification scheme

According to the simulation result of the first modification scheme, the metal flow of part 2 needs to be further improved. In the second modification scheme, the structural dimension of baffle plate 2 is further optimized. Keeping the same height as the first modification scheme and expanding the distance between the baffle plate 2 and the die orifice, with the size of the welding chamber enlarged to increase the material supply, the modification details are shown in Fig. 9. Figure 10 shows the velocity distribution in the cross-section after the second modification. As can be seen, on the basis of the first modification, the velocity range is further reduced (47.2–38.5 mm/s), the SDV value is found to be 3.5 mm/s, and there is 42.6% decrease before optimization. After two modifications, the velocity distribution in the cross-section of the profile becomes more reasonable, and could be applied in the actual extrusion production.

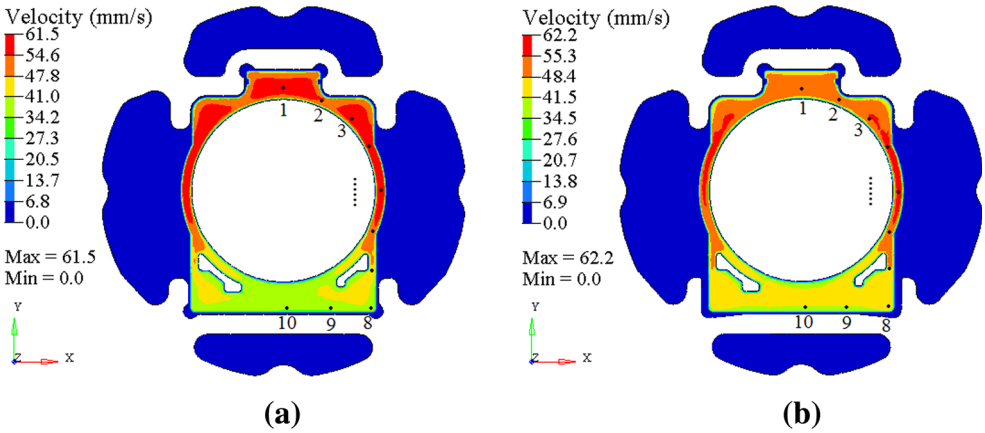

Fig. 11 Comparison of the material velocity at the inlet of die orifice. **a** The initial die design. **b** The optimum die design

4.3 Comparison and discussion of the initial and optimum die design

Figure 11 shows the velocity distribution at the inlet of die orifice before and after modification of the extrusion die. As can be seen, the metal flow velocity at the inlet of die orifice becomes more uniform after modification. The velocity in the part 2 zone increases, while it has decreased in the part 1 zone. In this section, ten reference points are selected as the evaluation objects as shown in Fig. 11. Figure 12 shows the velocity curves of the reference points before and after modification. It is seen that the difference in velocity at the inlet of die orifice is significantly reduced with the optimum die design. The results show that the metal flow can be effectively controlled by adjusting the shape and size of the baffle plate.

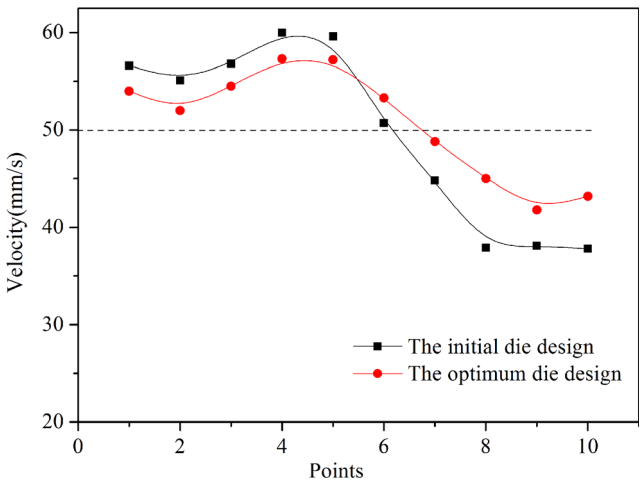

Fig. 12 Velocity curves of the reference points

5 Experiments and discussions

The real extrusion die is manufactured according to the optimal design as shown in Fig. 13. The extrusion process parameters adopted in the actual production are exactly the same as the numerical simulations, and the actual extruded profile is shown in Fig. 14a. As can be seen, no distinct bend, twist deformation, and dimension errors were found in the cross-section.

Fig. 14b shows the distribution of grain sizes of the profile section. As can be seen in Fig. 14b, the grain size distribution is uneven. The grain sizes at part B are the largest, followed by the smaller ones at part A, and the smallest ones at part C. The photographs of microstructures in these parts on the cross-section of the profile are shown in Fig. 14c, d, e. The average grain sizes are about 210, 250, and 88 μm, respectively, and the distribution trend is basically consistent with the simulation results.

Figure 15 shows the distribution of grain sizes at the inlet of die orifice. Similar to the grain distribution on the cross-section of the profile in Fig. 14b, the grain sizes at the thin wall on both sides of the cavity are relatively small. Figure 16 shows the distribution of strain rate at the inlet of die orifice. It can be found that the strain rate distribution is not uniform and the strain rate at the thin wall is larger than that at the thick wall. Ten reference points are selected as the evaluation

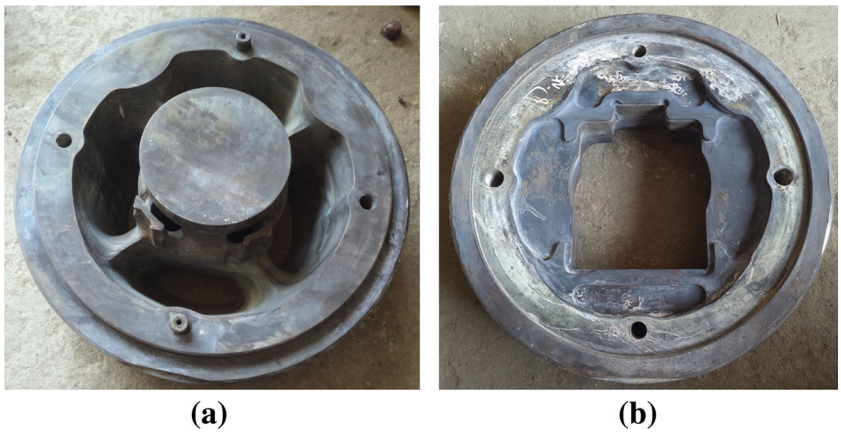

Fig. 13 Photographs of the real extrusion die. **a** Upper die. **b** Lower die

objects. The curves of strain rate and grain size of the reference points are shown in Fig. 17. It can be seen that the two curves are approximately symmetric to the dashed line. Constrained by the shape of die orifice, the deformation degree of the material at the thin wall is larger. Correspondingly, the strain rate is larger and the grain refinement degree is significant. In fact, the shape of die orifice is determined by the shape of the product section. Therefore, the uneven deformation caused by the difference in wall thickness of the product section is the main factor that causes the not uniform distribution of grain sizes in the cross-section of the product.

Figure 18 shows the temperature distribution of the material in the die cavity in the four different periods. Fig. 18a depicts the temperature distribution of the material in portholes. As can be seen from Fig. 18a, compared to the four large portholes, the temperature in the two small portholes is relatively high because more quantity of heat is generated due to the greater degree of deformation. In the four large portholes, the frictional resistance between the outer material and the inner wall of the portholes makes the outer material mainly subjected to shear deformation and the deformation degree from outer to inner is gradually reduced, thereby the

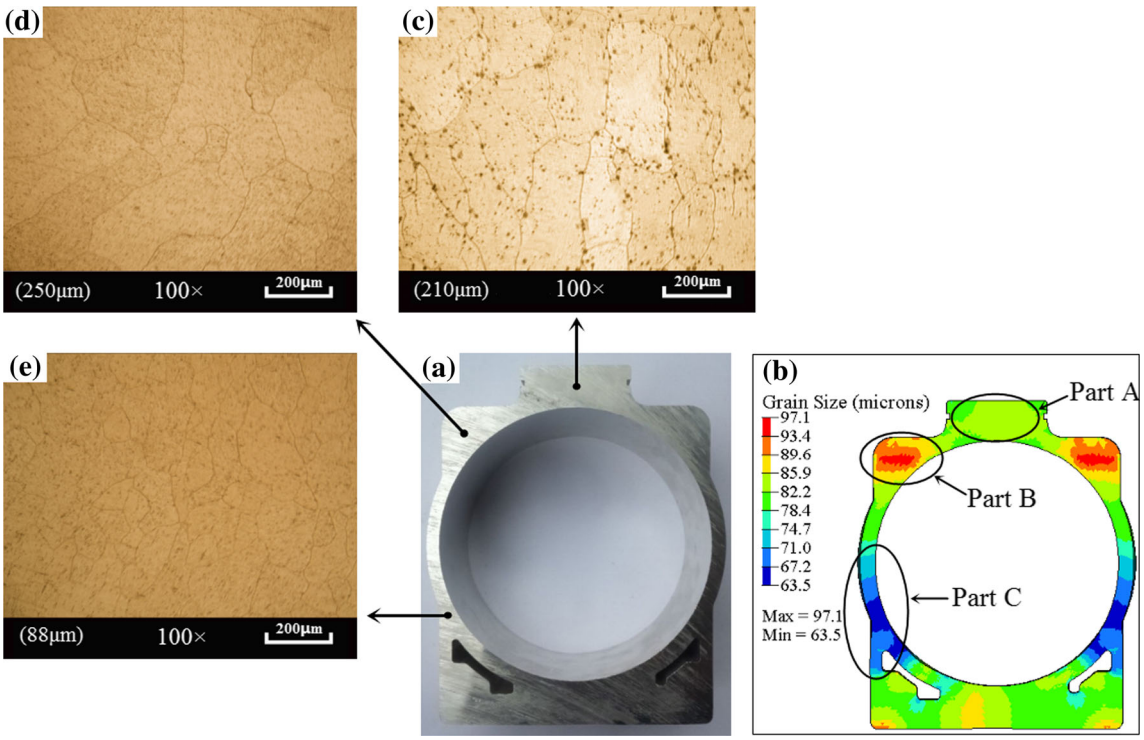

Fig. 14 Photographs of the profile and microstructures of the product. **a** The profile. **b** Distribution of grain sizes of the profile section; **c** microstructure at *part A*. **d** Microstructure at *part B*. **e** Microstructure at *part C*

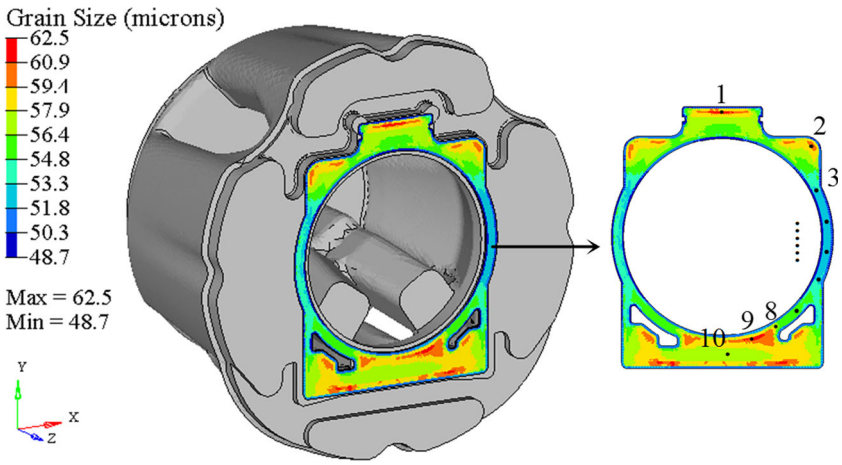

Fig. 15 Distribution of grain sizes at the inlet of die orifice

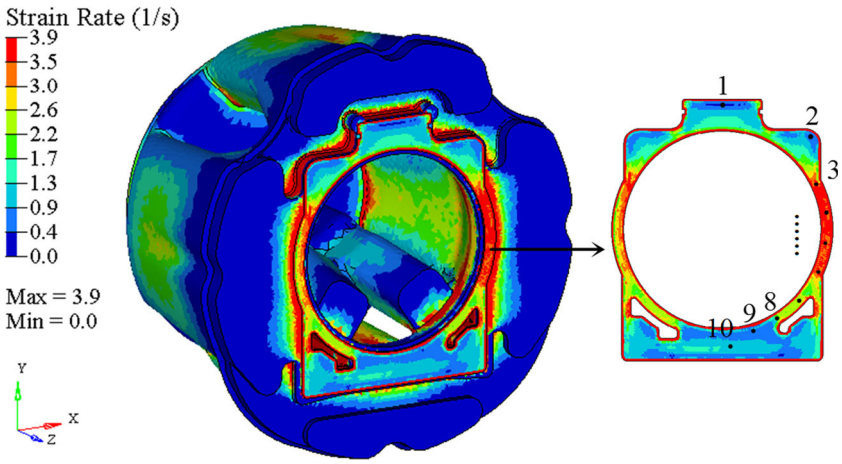

Fig. 16 Distribution of strain rate in the die cavity

friction heat decreases gradually. As a result, the temperature at the portholes center is lower than that at the surrounding area.

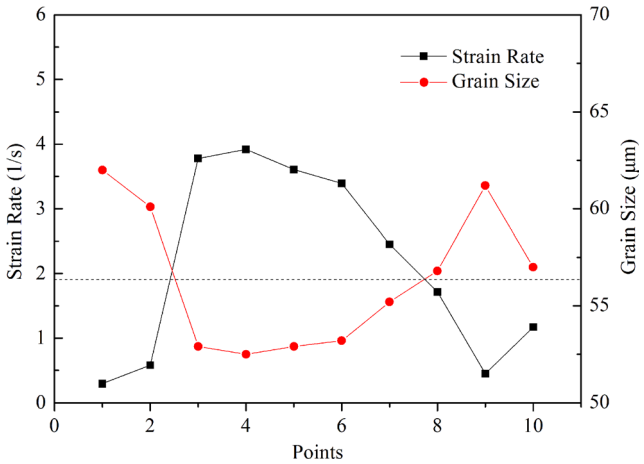

Fig. 17 Strain rate curve and grain size curve of the reference points

Fig. 18b–d show the temperature distribution of the material in the welding chamber at three different stages. It can be found that the material begins to weld below the porthole bridges. As the welding process progresses, the temperature on the welding lines is always high for the reasons given above.

After the material flows out of the die orifice, the extruded profile is no longer subjected to external forces. The grains grow under the influence of temperature. The temperature distribution of the profile is shown in Fig. 19. The temperature is unevenly distributed on the profile under the effect of the welding process shown in Fig. 18. In the cross-section of the profile, the temperature around the welding lines is higher than that at the thin walls. It can be seen from Figs. 14b and 15, as the material is extruded from the die orifice, the grain growth rate around the welding lines (part B) is faster than that is in part A and C, while it is the lowest at the thin walls (part C).

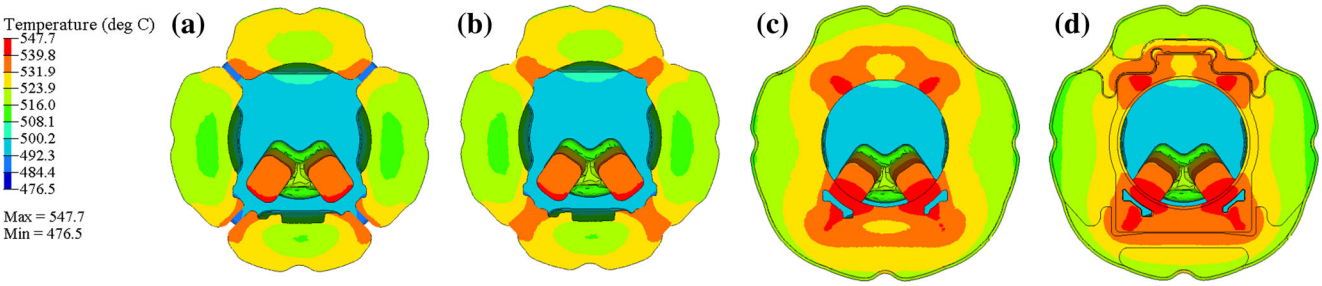

Fig. 18 Temperature distribution of the material. **a** In portholes. **b** The beginning of welding. **c** The middle of welding, **d** The end of welding

6 Conclusions

In this paper, the extrusion process of a hollow aluminum profile with a large difference in wall thickness has been investigated by means of numerical simulation and physical experiments. By adjusting the height and shape of baffle plate, a profile with desired shape and size has been obtained. The microstructure distribution of the product section has been analyzed numerically. The main conclusions are as follows:

1. In the extrusion process of profiles with a large difference in wall thickness, baffle plates play an important role in balancing the metal flow and material distribution. By adjusting the shape and size of baffle plate, the velocity distribution in the cross-section of the profile becomes more uniform. The SDV is found to be 3.5 mm/s with the optimum die, and there is 42.6% decrease in SDV compared with the initial die scheme.
2. A real extrusion die is manufactured according to the optimal design and the extruded profile satisfies the practical requirements. The modified design of baffle plate based on the numerical simulation has been proved to be efficient for the optimization of complex die design and provides guidelines for the extrusion production of large and complex hollow aluminum profiles.
3. There is an uneven distribution of grain sizes in the cross-section of the profile and the distribution trend is greatly consistent with the simulation results. The results show that the uneven deformation caused by the difference in wall thickness is the main factor that causes the uneven distribution of grain sizes in the cross-section of the product. When the material flows out of the die orifice, the grain growth rates are different under the influence of the uneven temperature distribution on the profile section.

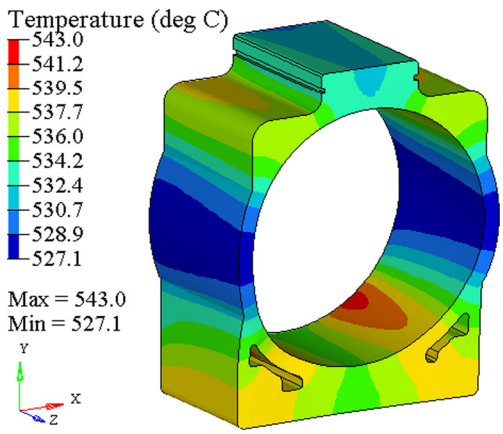

Fig. 19 Temperature distribution of the profile

References

1. Chen L, Zhao GQ, Yu JQ (2015) Effects of ram velocity on pyramid die extrusion of hollow aluminum profile. Int J Adv Manuf Technol 79:2117–2125
2. Zhang CS, Yang S, Wang CX, Zhao GQ, Gao AJ, Wang LJ (2016) Numerical and experimental investigation on thermo- mechanical behavior during transient extrusion process of high-strength 7××× aluminum alloy profile. Int J Adv Manuf Technol 85:1915–1926
3. Chen H, Zhao GQ, Zhang CS, Guan YJ, Liu H, Kou FJ (2011) Numerical simulation of extrusion process and die structure optimization for a complex aluminum multicavity wallboard of high-speed train. Mater Manuf Process 26:1530–1538
4. Zhang CS, Zhao GQ, Chen ZR, Chen H, Kou FJ (2012) Effects of extrusion stem speed on extrusion process for a hollow aluminum profile. Mater Sci Eng B 177:1691–1697
5. Lee JM, Kim BM, Kang CG (2005) Effects of chamber shapes of porthole die on elastic deformation and extrusion process in condenser tube extrusion. Mater Des 26:327–336
6. Wu XH, Zhao GQ, Luan YG, Ma XW (2006) Numerical simulation and die structure optimization of an aluminum rectangular hollow pipe extrusion process. Mater Sci Eng A 435–436:266–274
7. He YF, Xie SS, Chen L, Huang GJ, Fu Y (2010) FEM simulation of aluminum extrusion process in porthole die with pockets. Trans Nonferrous Metals Soc China 20:1067–1071
8. Dong YY, Zhang CS, Zhao GQ, Guan YJ, Gao AJ, Sun WC (2016) Constitutive equation and processing maps of an Al–Mg–Si aluminum alloy: determination and application in simulating extrusion process of complex profiles. Mater Des 92:983–997

9. Zhang CS, Zhao GQ, Guan YJ, Gao AJ, Wang LJ, Li P (2015) Virtual tryout and optimization of the extrusion die for an aluminum profile with complex cross-sections. Int J Adv Manuf Technol 78: 927–937
10. Luo S, Wu XK (2006) Aluminum profiles extrusion applied technical manual. Central South University, Hunan
11. Liu JA, Shao LF (2007) Aluminum alloy extrusion mold typical atlas. Chemical Industry, Beijing
12. Zhang CS, Zhao GQ, Chen H, Guan YJ, Li HK (2012) Optimization of an aluminum profile extrusion process based on Taguchi's method with S/N analysis. Int J Adv Manuf Technol 60: 589–599
13. Guan YJ, Zhang CS, Zhao GQ, Sun XM, Li P (2012) Design of a multihole porthole die for aluminum tube extrusion. Mater Manuf Process 27:47–53
14. Yu JQ, Zhao GQ, Chen L (2016) Investigation of interface evolution, microstructure and mechanical properties of solid-state bonding seams in hot extrusion process of aluminum alloy profile. J Mater Process Technol 230:153–166
15. Chen ZZ, Lou ZL, Ruan XY (2007) Finite volume simulation and mould optimization of aluminum profile extrusion. J Mater Process Technol 190:382–386